Journal of Physics: Conference Series **628** (2015) 012074 doi:10.1088/1742-6596/628/1/012074

Use of high frequency analysis of acoustic emission signals to determine rolling element bearing condition

A Cockerill[1], K M Holford[1], T Bradshaw[2], P Cole[2], R Pullin[1] and A Clarke[1]

[1] *School of Engineering, Cardiff University, UK, CF24 3AA*
[2]*Mistras Group Limited, Over, Cambridge, UK, CB24 5QE*

Email: *CockerillA@cardiff.ac.uk*

Abstract: Acoustic Emission (AE) sensors were used to detect signals arising from a cylindrical roller bearing with artificial defects seeded onto the outer raceway. An SKF N204ECP roller bearing was placed between two double row spherical roller bearings, type SKF 22202E, and loaded between 0.29 and 1.79kN. Speed was constant at 5780rpm. High frequency analysis allowed insight into the condition of the bearings through the determination of an increase in the structural resonances of the system as the size of an artificial defect was increased. As higher loads were applied, frequencies around 100kHz were excited, indicating the release of AE possibly attributed to friction and the plastic deformation as peaks, induced through engraving of the raceway, were flattened and worn down. Sensitivity of AE to this level in bearings indicates the potential of the technique to detect the early stages of bearing failure during life tests.

INTRODUCTION

Rolling element bearings are found within machinery in a wide variety of industries including the aerospace, automotive and renewable energy sectors. Failure of such bearings can lead to costly asset downtime or at worst, catastrophic failure and the loss of human life. Although bearings are designed with longevity in mind, it has been calculated that approximately 10% of bearings will fail before reaching their predicted life, L_{10}, as derived by Lundberg and Palmgren [1]. In real world applications, the bearing can be significantly overloaded, vastly reducing the number of cycles that the bearing can sustain. This, coupled with variation in operational temperature, oil cleanliness and lubrication regime, make it very difficult to predict with confidence when or how a bearing will fail due to fatigue. With advancing research in the areas of tribology and condition monitoring, it is now possible to detect incipient damage on bearing raceways and rolling elements before complete bearing failure occurs [2].

Of the condition monitoring techniques available, vibrational analysis has been widely adopted within industry to detect defects within rotating machinery [3]. It is well understood that the repeatable passing of the rolling elements over the point of maximum load produces characteristic frequencies directly associated with the geometry and specifications of the bearing itself [4]. The characteristic frequencies have long been used to determine the location of a bearing defect where an increase in frequency amplitude over time is attributed to an increase in defect severity. Although this provides a

good indication of a defects existence, when this method is applied to heavy machinery operating with a large amount of low frequency noise and high inertia, the low amplitude defect frequencies of small defects can often be masked [5][6]. Complex transmission paths also result in a large attenuation of a defect signal making it difficult to detect a defect in its earliest stages. Although weak signal extraction methods can be used, the time between defect detection and machine failure can still be relatively small [5]. This is inherent in the use of vibration techniques that detect the response of a structure to a defect rather than the occurrence and growth of the defect itself. As an alternative to vibrational analysis, Acoustic Emission (AE) is proposed as a more sensitive technique to detect early-stage damage within rotating machinery. AE is the detection of transient elastic waves caused by plastic deformation, crack tip growth, fluid flow, sharp impacts, friction/rubbing and fractures/dislocations of fibres and is commonly used to detect damage in static structures such as bridges and pressure vessels. For bearings it is thought that AE is induced through sub-surface and surface cracking, friction and plastic deformation of surface asperities during the running in phase and rolling fatigue failure [7]. As a crack grows, a short burst of high frequency energy is released and transmitted through the structure until it propagates to the surface and is detected by a sensor [8]. A benefit of using AE over vibration is its signal to noise ratio. Most rotating machinery operates in the low frequency range (sub 20kHz) but AE is sensitive from 50kHz-1MHz. This allows AE sensors to detect frequencies both in the vibration spectrum as well as the high frequency components, currently unable to be detected by traditional accelerometers.

Most analysis of AE data focuses on basic characteristics or parameters that are calculated from the raw signal, such as Root Mean Square (RMS), hits and counts. Although able to determine bearing condition holistically, use of techniques such as RMS presents difficulty when trying to identify the failure mechanism occurring within the bearing. Pullin *et al.* determined the crack growth of a spur gear tooth by monitoring the frequency response from an AE sensor over a period of time [8]. Howard [9] states that the three important steps of condition monitoring are detection, diagnosis and prognosis. The work presented in this paper investigates how RMS, high frequency analysis and characteristic defect frequencies can be used together to detect and diagnose the condition of artificially damaged bearings.

EXPERIMENTAL SET UP

2.1 Test Head

Figure 1 illustrates the bearing test head that was driven by a 0.55kW motor at a speed of approximately 5780rpm through a timing belt pulley. The test bearing (1) is situated between two support bearings (2) and the 10:1 lever arm (3) is used to apply a radial load directly to the test bearing. The two spherical roller support bearings, type SKF 22205/20E, were selected due to their high fatigue load capacity. The cylindrical roller test bearing, type SKF N204ECP, was selected due to the simplicity in the separation of the bearing into its constituent parts. All bearings are 20mm inner raceway bore. Table 1 shows the characteristic frequencies of the bearings used for a shaft frequency of 97.83Hz (5780rpm). Since the support bearings only see half of the load experienced by the test bearing, any damage is highly likely to occur solely in the test bearing.

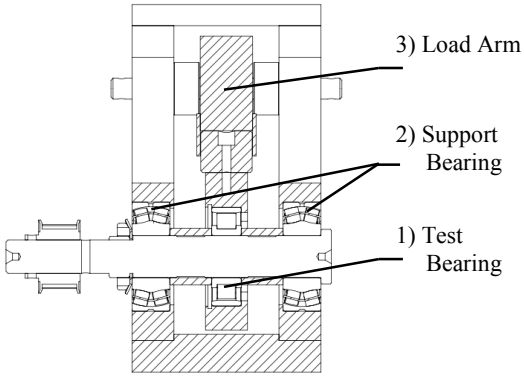

Figure 1) Test Head Schematic

Table 1. Determination of Characteristic Frequencies

Defect Frequencies	**N204ECP**	**22202/20E**
Outer (Hz)	419.4	604.5
Inner (Hz)	656.7	863.0
Ball Spin (Hz)	211.0	262.3
Train (Hz)	38.1	40.3

Each bearing was lubricated via individual oil jet feeds with a mineral oil (meeting OEP-80 performance specification) supplied at 50°C. For the healthy bearing, five radial loads were applied: HL1, HL2, HL3, HL4 and HL5 which represent 0.29, 0.61, 1.29, 1.61 and 1.8kN respectively. For the damaged bearing four loads were applied: L1, L2, L3 and L4, representing 0.29, 0.79, 1.29 and 1.8kN respectively.

2.2 Data Acquisition

Mistras Group Limited (MGL) Nano30 AE sensors were placed onto the bearing housings, close to the outer raceway of each bearing. Lithium-based grease was applied as a couplant to improve the transmission of the signal from the test head into the sensor. Magnets were used to secure the sensors into position. Each sensor was connected to an amplifier with 40db gain and a bandpass filter of 20-1500kHz. Nano30 sensors were selected due to their small size and high resonant frequency of 300kHz whilst maintaining reasonable bandwidth. A MGL PCI-2 system was used to collect manually triggered waveforms at a sampling frequency of 2MHz. Before waveforms were recorded, the test head was run until steady state temperatures were achieved for all bearings. For each load, a total of four waveforms were recorded at intervals of 2,000 revolutions. The load was then increased and the next four waveforms were taken after approximately 10,000 revolutions, counted by an optical revolution counter mounted on the test shaft.

2.3 Seeded Defects

To replicate common bearing failure modes, artificial defects were engraved onto the outer raceway of the test bearing. Before and after each test, the defect was measured using a Taylor Hobson Talysurf surface profilometer. Artificial defects are by no means a direct replication of natural damage propagation seen in bearings. It is common for sub-surface cracks to initiate due to the stresses induced as the rolling element passes over the point of maximum load [7]. As these cracks grow, they can propagate to the surface of the raceway causing pieces of material to dislodge. Engraving the surface does not remove material but instead creates an engraved pit surrounded by peaks as the material is forced upwards. Although not a true representation of the failure modes of a bearing, engraving allows for quick validation of the equipment and methodology before conducting life tests as well as demonstrating the sensitivity of AE for use within rotating machinery to detect realistically sized defects. Table 2 quantifies the size of each of the seeded defects through the determination of the volume of the peaks and the troughs created through engraving using the least squares method.

Table 2. Defect Volumes

	Defect 1	Defect 2	Defect 3	Defect 4	Defect 5	Defect 6
Peak (mm^3)	2.62E-004	1.05E-003	5.76E-003	6.56E-003	5.36E-003	1.44E-002
Valley (mm^3)	2.62E004	1.06E-003	5.76E-003	6.56E-003	5.34E-003	1.45E-002

3. RESULTS AND DISCUSSION

Figure 2 is the RMS_{AE} vs. load for each of the seeded defects. Defect 1 and defect 2 are both point defects in the centre of the outer raceway and show a large rise in the RMS_{AE} value compared to the healthy bearing. As the defect is expanded from a point defect to multiple points across the width of the bearing, defect 3, a large reduction in the RMS_{AE} is seen, although the amplitude of the RMS_{AE} remains higher than that of the undamaged bearing. As the depth and width of the defect is increased from defect 3 to defect 6, the RMS_{AE} continued to increase. The significant reduction in RMS value between defect 2 and defect 3 is considered to be due to an increase in contact area as the defect is spread across the raceway. The RMS value indicates that the AE generated by each defect depends on the defect size, but little information can be determined about what is happening within the bearing itself.

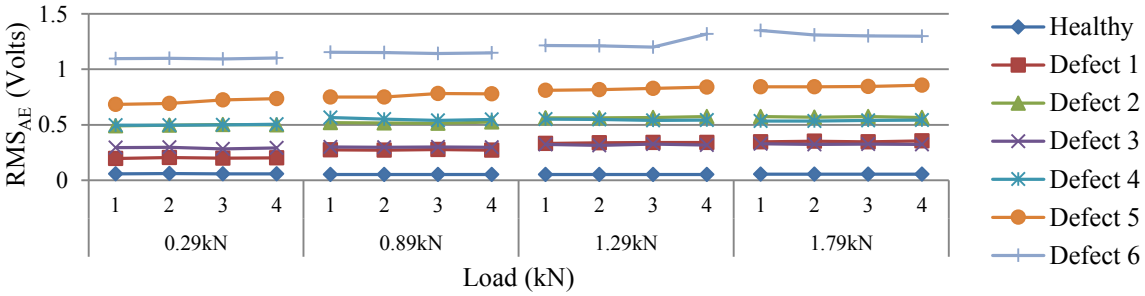

Figure 2) Comparison of RMS values of healthy and damaged bearings

For each collected waveform, a Fast Fourier Transform (FFT) was calculated and plotted against time to produce a 3-dimensional graph. In order to smooth the data for easier interpretation, the x-axis was separated into a number of frequency bands, or bins, where each bin is the sum of all of the frequency amplitudes within. Figure 3a and 3b are stacked FFT's between 0-75kHz and 75-150kHz respectively for a healthy bearing with a bin width of 20Hz. The y-axis is divided into the separate loads applied where each load contains the four collected waveforms, demonstrating amplitude fluctuation over time.

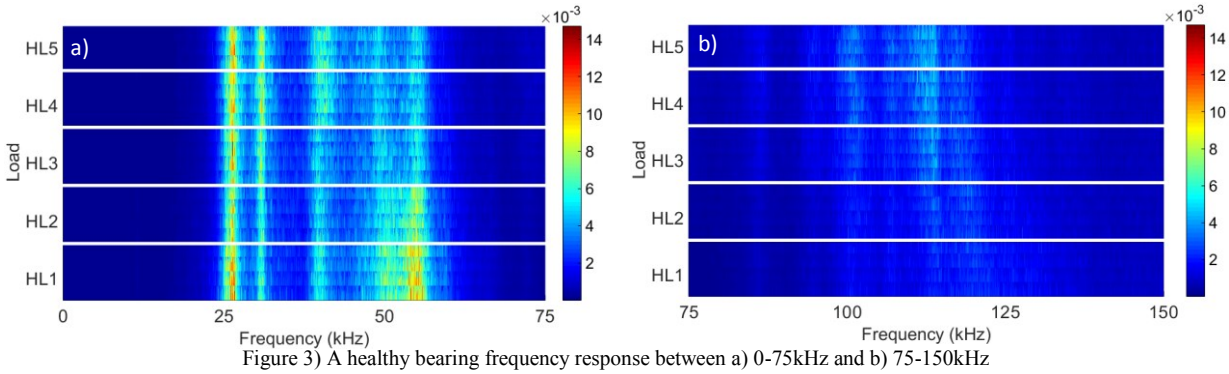

Figure 3) A healthy bearing frequency response between a) 0-75kHz and b) 75-150kHz

It can be seen that the dominant frequency within the healthy bearing signal is around 26kHz. It is thought that the value of 26kHz relates to either the structural resonance of the test housing or of the bearing itself [10][11]. Since the resonant frequency of the Nano30 sensor is 300kHz, to excite the piezoelectric crystal in such a way a significant amount of energy must be present at 26kHz. Figure 3a also shows significant energy at approximately 60 kHz for loads HL1 and HL2. Between HL3 and HL5 the amplitude around 60kHz decreases and the amplitude around 35 kHz increases. This could be due to the system being damped as the load is increased or even evidence of the end of the running in phase. Figure 3b illustrates that higher frequency AE can also be witnessed as the load is increased. Energy in the frequency band of 100-125kHz is indicative of AE sources occurring within the bearing. It is thought that the high frequency emission seen in a healthy bearing is induced through friction between the roller and the races as the bearing completes its 'running in' phase. During the running in phase, surface roughness asperities are smoothed over as the rollers pass over in quick succession. This flattening of the raceways requires plastic deformation of asperities and is therefore a likely source of high frequency emission.

Figures 4(a-f) are low frequency (0-75kHz) stacked FFT's of defects 1-6. The suspected system resonances excited are at similar frequencies to those witnessed within the healthy bearing, albeit at an order of magnitude higher in amplitude. As the defect size increases the magnitude of the resonant frequencies increase dramatically. This increase in amplitude of the resonant frequencies could be used to determine the severity of the defect or be used to demodulate the signals to help ease weak signal extraction. Figure 5(a-f) illustrates the high frequency (75-150kHz) stacked FFT's of defects 1-6. Unlike the low frequency stacked FFT's, an increase in amplitude can be seen as the load increased.

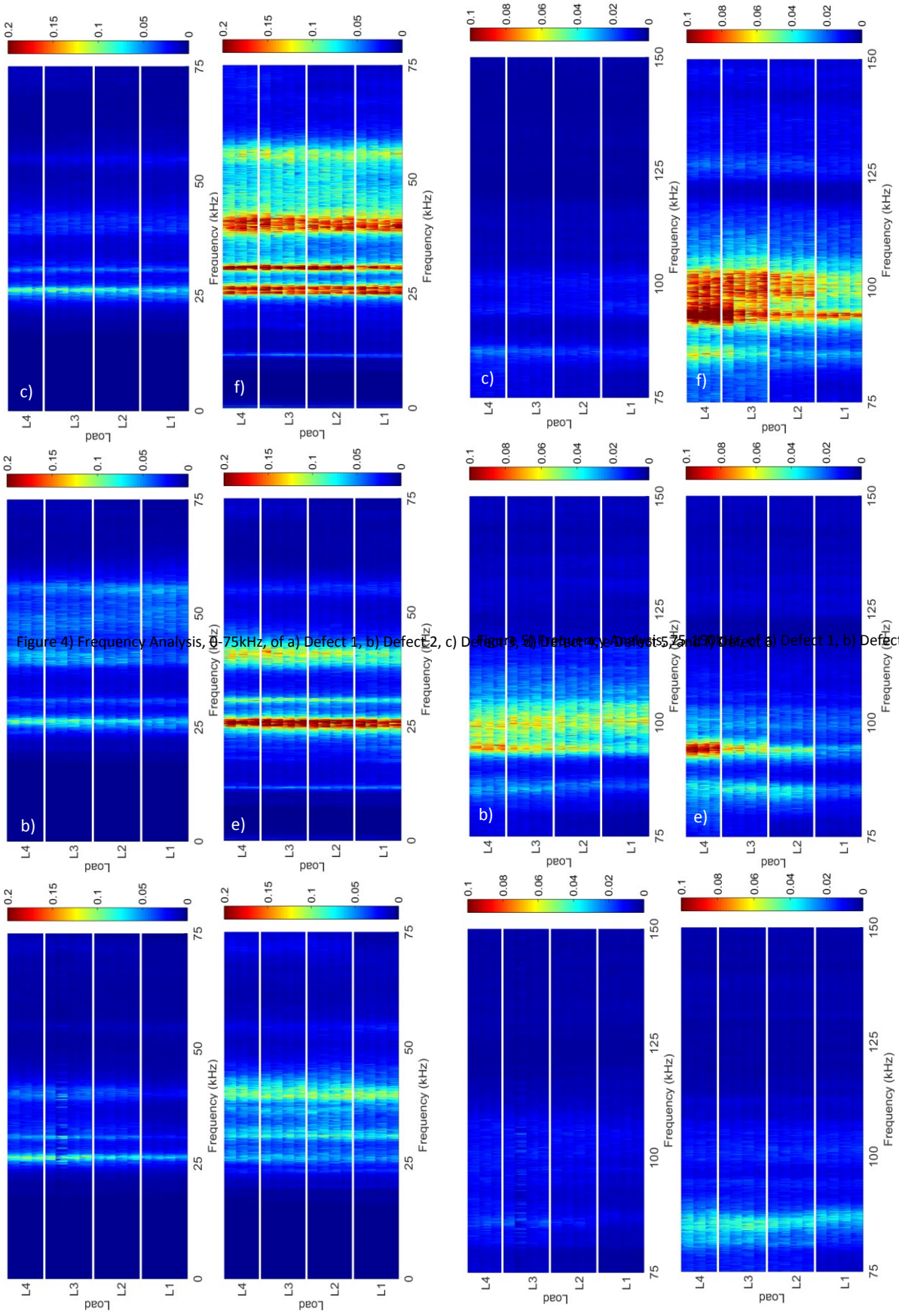

Figure 4) Frequency Analysis, 0-75kHz, of a) Defect 1, b) Defect 2, c) Defect 3, d) Defect 4

Figure 5) Frequency Analysis, 75-150kHz, of a) Defect 1, b) Defect 2, c) Defect 3, d) Defect

It is thought that these high frequency components are caused as the rollers pass over the sharp peaks of the seeded defects, as well as friction between the interacting bodies. Similar to the high frequency AE that occurs during crack growth, high localised stresses within the area of contact cause the peaks to become plastically deformed or to fracture. Evidence of this can be seen in Figure 6 where a pre and post-test measurement of defect 2 are compared together. It can be seen that the sharp peaks witnessed in the pre-test measurement are plastically deformed and flattened significantly during the test.

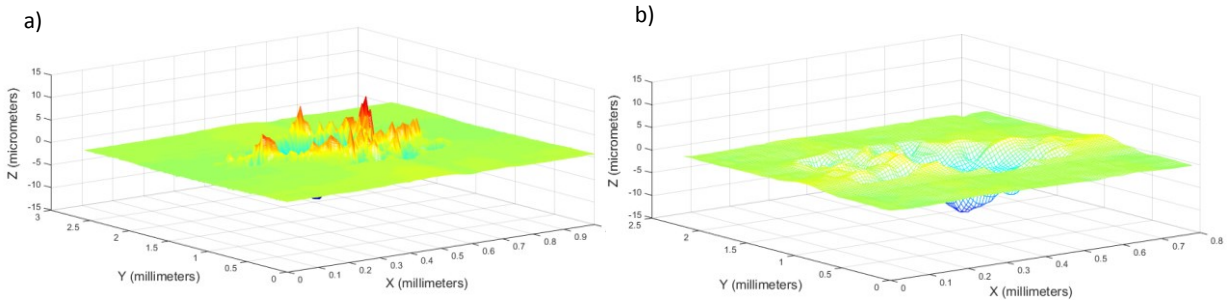

Figure 6) a) Pre-Test surface measurement and b) Post-Test surface measurement

During the natural degradation of bearing raceways, there are rarely any sharp peaks surrounding pits in the surface as material tends to become dislodged from the surface as opposed to being forced upwards as occurs in the artificial defects used in this work. Any sharp edges of a naturally occurring defect would become quickly flattened and smoothed during the repeated over-rolling in the life of a bearing. Figure 5 demonstrates that the high frequency acoustic emission released from the bearing raceway can be detected at the surface of the bearing housing. Therefore, it is hoped that the AE released during the natural fatigue of the bearing surface during a life test to failure will be detectable using similar techniques.

The RMS value indicates gross bearing change and the stacked FFT illustrates the detailed nature of the interaction between rollers and defects within the bearings. With such a large number of possible failure mechanisms within a bearing, the location at which a defect is propagating is of importance as the attenuation from the inner raceway is far more severe than from the outer raceway. For a sensor mounted on the stationary outer race bearing housing, an AE wave from the inner race has to pass through two elastohydrodynamic oil films, and through two additional solid bodies (roller and outer race) before it reaches the sensor. To determine location, the characteristic defect frequencies determined in Table 1 are used. Figure 7 is the raw waveform and FFT of a healthy bearing. The low frequency response has low amplitude and is dominated by orders of shaft rotation with no other dominant frequency spikes. A similar signal and frequency response is witnessed for defect 1 albeit with larger amplitudes (Figure 8).

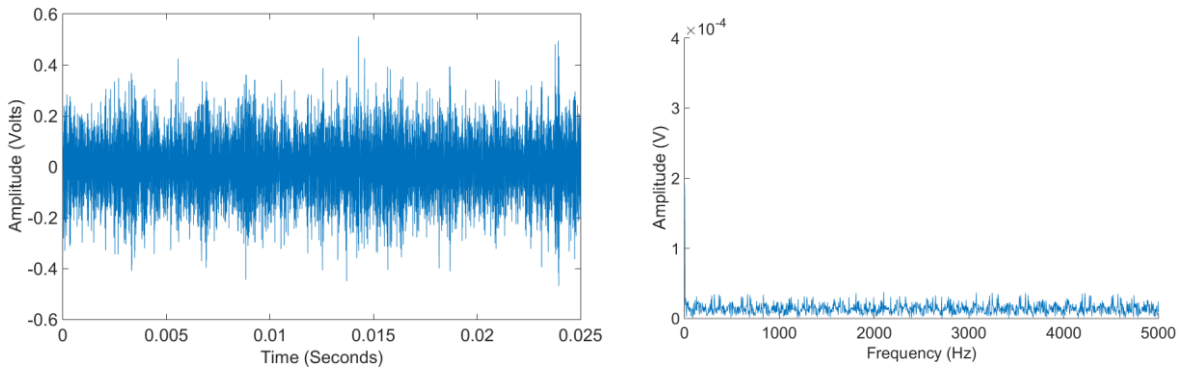

Figure 7) The raw waveform and FFT of a healthy bearing

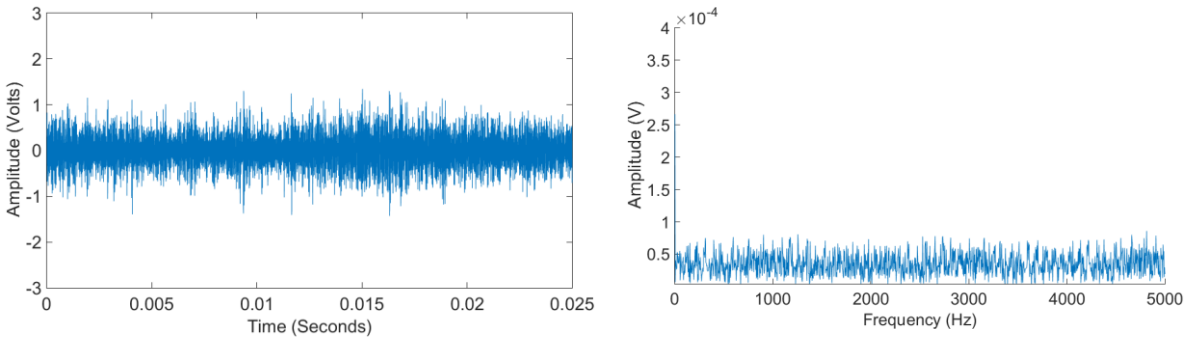

Figure 8) The raw waveform and FFT of defect 1

As the size of the defect is increased from defect 1 to defect 2, repeatable high frequency bursts are witnessed within the raw waveform (Figure 9). These bursts occur close to the outer race defect frequency of 415.8Hz as shown in the FFT. As the damage size is increased to the maximum of defect 6, the amplitude of the outer race defect frequency within the FFT becomes more apparent and multiple orders are witnessed within the FFT (Figure 10).

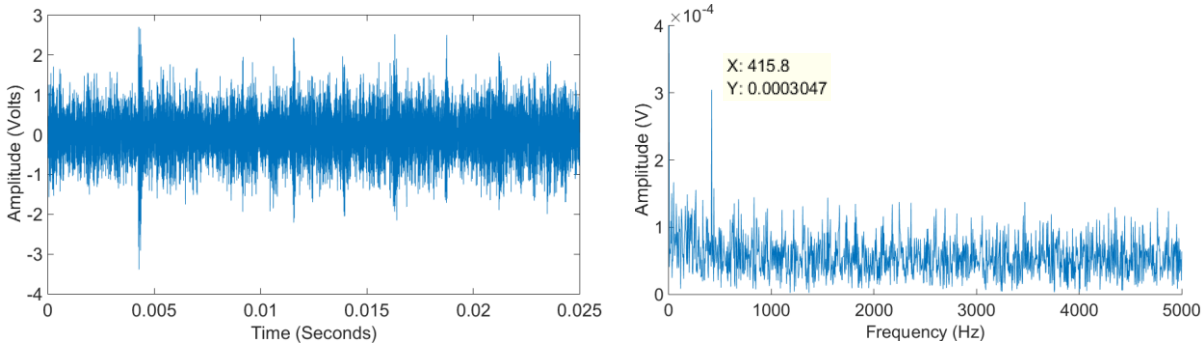

Figure 9) The raw waveform and FFT of defect 2

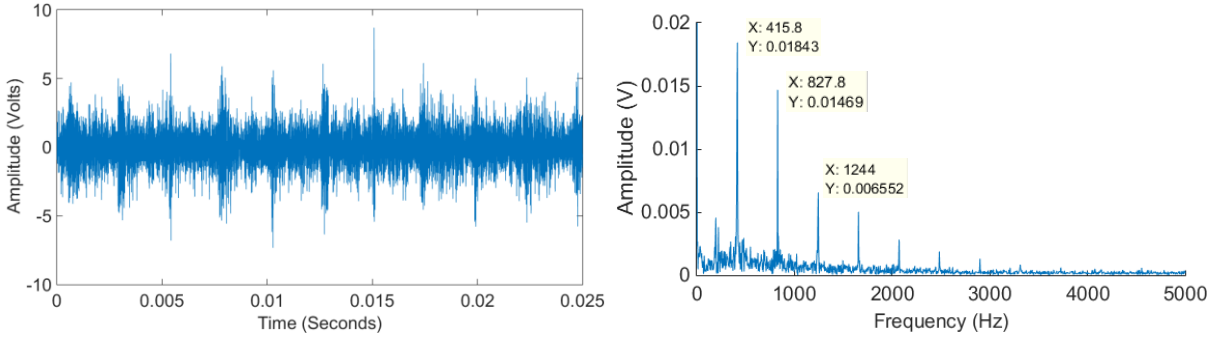

Figure 10) The raw waveform and FFT of defect 6

Although bearing defect frequencies are commonly relied upon in the condition monitoring of bearings with both vibrational and AE signals, Figure 11b is the frequency response from an AE sensor mounted upon a support bearing during the analysis of defect 6. It can be seen that a frequency close to the outer raceway defect frequency of the support bearing, (approx. 605Hz), has increased amplitude when compared with its healthy counterpart Figure 11a. It is thought that the damage of the test bearing is exciting the characteristic frequencies of the support bearing. Current condition monitoring techniques may represent this bearing as being damaged however, post-test inspection of this bearing showed the outer raceway to be unmarked and visually healthy.

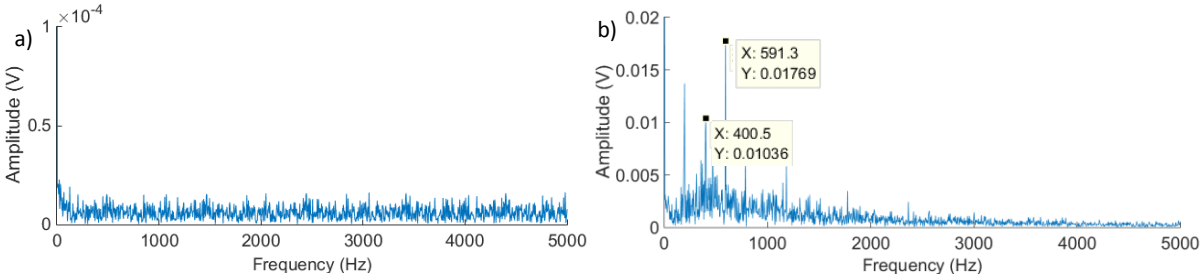

Figure 11) The FFT of the support bearing of a) a healthy bearing and b) defect 6

4. CONCLUSION

Seeded defects placed upon the outer raceway of a rolling element bearing were detectable through RMS and frequency analysis, in both low and high frequency ranges. As the defect spreads across the raceway, the amount of energy released reduces and this can be seen in both the high frequency response and the RMS values. Thus the size and shape of the defect has a large influence on the release of AE from it. The high frequency analysis has determined that as the defect size increases, the structural frequencies are excited without a significant change as the load is increased. The high frequency components, (75-150kHz), do increase in magnitude with an increase of load and therefore it is deduced that the change in this high frequency section is most likely to be due to plastic deformation occurring as the rollers pass over sharp peaks produced by engraving.

Acknowledgements

The authors wish to acknowledge the support of EPSRC Grant references EP/L021757/1, and EP/K031635/1 which facilitated this work in part. The first author acknowledges the financial support of Mistras Group Limited towards his studentship.

References

[1] Lundberg G and Palmgren A 1952 Dynamic capacity of roller bearings Acta Polytech Mechanical Engineering Series, 2.
[2] Halme J and Andersson P 2010 *Proceedings of the Institution of Mech. Eng. Part J: J. Eng. Tribology* **224(4)** 377–393
[3] García Márquez F P, Tobias A M, Pinar Pérez J M and Papaelias M 2012 *Renewable Energy* **46** 169–178.
[4] Harris T A and Kotzalas M N 2006. Essential concepts of bearing technology CRC press
[5] Qiu H, Lee J, Lin J and Yu G 2003 *Advanced Engineering Informatics* **17(3-4)** 127–140
[6] Ho D and Randall R B 2000 Mech. Systems & Sig Processing **14(5)** 763-788.
[7] Lees A W, Quiney Z, Ganji A and Murray B 2011 *J. Phys. Conf. Series* **305** 012074
[8] Pullin R, Clarke A, Eaton M J, Pearson M R and Holford K M 2012 *J. Phys: Conf. Series* **382(1)** 2050
[9] Howard I 1994 *A Review of Rolling Element Bearing Vibration 'Detection, Diagnosis and Prognosis'*. No. DSTO-RR-0013. DEFENCE SCIENCE AND TECHNOLOGY ORGANIZATION CANBERRA (AUSTRALIA)
[10] Tandon N and Choudhury A 1999 *Tribology international* **32** 469-480
[11] Rai V K and Mohanty A R 2007 *Mech. Systems & Sig. Processing* **21(6)** 2607-2615